

https://doi.org/10.1093/g3journal/jkad257 Advance Access Publication Date: 10 November 2023

Investigation

# Massive contractions of myotonic dystrophy type 2-associated CCTG tetranucleotide repeats occur via double-strand break repair with distinct requirements for DNA helicases

David Papp,<sup>1</sup> Luis A. Hernandez,<sup>1</sup> Theresa A. Mai,<sup>1</sup> Terrance J. Haanen,<sup>1</sup> Meghan A. O'Donnell,<sup>1</sup> Ariel T. Duran,<sup>1</sup> Sophia M. Hernandez,<sup>1</sup> Jenni E. Narvanto,<sup>1</sup> Berenice Arguello,<sup>1</sup> Marvin O. Onwukwe,<sup>1</sup> Sergei M. Mirkin , <sup>2</sup> Jane C. Kim , <sup>1</sup>\*

Myotonic dystrophy type 2 (DM2) is a genetic disease caused by expanded CCTG DNA repeats in the first intron of *CNBP*. The number of CCTG repeats in DM2 patients ranges from 75 to 11,000, yet little is known about the molecular mechanisms responsible for repeat expansions or contractions. We developed an experimental system in *Saccharomyces cerevisiae* that enables the selection of large-scale contractions of (CCTG)<sub>100</sub> within the intron of a reporter gene and subsequent genetic analysis. Contractions exceeded 80 repeat units, causing the final repetitive tract to be well below the threshold for disease. We found that Rad51 and Rad52 are involved in these massive contractions, indicating a mechanism that uses homologous recombination. *Srs2* helicase was shown previously to stabilize CTG, CAG, and CGG repeats. Loss of Srs2 did not significantly affect CCTG contraction rates in unperturbed conditions. In contrast, loss of the RecQ helicase *Sgs1* resulted in a 6-fold decrease in contraction rate with specific evidence that helicase activity is required for large-scale contractions. Using a genetic assay to evaluate chromosome arm loss, we determined that CCTG and reverse complementary CAGG repeats elevate the rate of chromosomal fragility compared to a short-track control. Overall, our results demonstrate that the genetic control of CCTG repeat contractions is notably distinct among disease-causing microsatellite repeat sequences.

Keywords: DNA repeats; microsatellites; DNA repair; homologous recombination

#### Introduction

Repeat expansion diseases are caused by excessively long tracts of simple DNA sequence repeats, also called microsatellites, within specific genes. Two types of myotonic dystrophy (DM) are examples of such diseases (Meola and Cardani 2015). DM1 is caused by long (>50) CTG trinucleotide repeats (TNRs) in the 3' UTR of DMPK, whereas DM2 is caused by long (>75) tetranucleotide CCTG repeats in the first intron of CNBP. Transcription of these expanded alleles results in cellular toxicity through RNA gain-offunction effects (Sznajder and Swanson 2019). Repeat-associated non-ATG translation products were observed in brain tissues of DM1 and DM2 patients (Zu et al. 2011, 2017), suggesting that aberrant proteins may also contribute to pathophysiology. Disease symptoms include the inability to relax muscles after they have contracted, muscle weakness, and cardiac conduction problems. However, no cure or specific therapy is currently available for either disease, with treatment relying on symptom management.

Individuals with DM1 or DM2 may have thousands of tandem repeats within the affected gene. Through studies using model organisms and cell culture systems, there have been substantial

advances in understanding CTG and reverse complementary CAG instability (expansions and contractions) (Usdin et al. 2015; Polyzos and McMurray 2017; Khristich and Mirkin 2020; Wheeler and Dion 2021). CAG/CTG repeats form stable hairpins and slipped strands in vitro, and the formation of these secondary structures in vivo is proposed to instigate various molecular mechanisms of instability (Pearson and Sinden 1998; Kim and Mirkin 2013; Poggi and Richard 2021). For example, polymerase slippage followed by hairpin formation on the nascent strand during DNA replication or repair synthesis would lead to an expansion. In contrast, structure formation on the template strand, which is then bypassed during DNA synthesis, would result in repeat contractions. Additionally, CAG/CTG repeats cause replication fork stalling (Fouche et al. 2006; Kerrest et al. 2009) and elevated DNA double-strand break (DSB) formation (Callahan et al. 2003; Polleys and Freudenreich 2020), and their recovery or repair via homologous recombination (HR) could lead to expansions or contractions depending on the fidelity of steps such as strand annealing (Polleys and Freudenreich 2021).

Understanding the molecular mechanisms of contractions is important to evaluate whether manipulating this process would

<sup>&</sup>lt;sup>1</sup>Department of Biological Sciences, California State University San Marcos, San Marcos, CA 92078, USA

<sup>&</sup>lt;sup>2</sup>Department of Biology, Tufts University, Medford, MA 02155, USA

<sup>\*</sup>Corresponding author: Department of Biological Sciences, California State University San Marcos, 333 S. Twin Oaks Valley Road, San Marcos, CA 92096, USA. Email: jckim@csusm.edu

be a viable approach to treat repeat expansion diseases (Izzo et al. 2022). Strategies to induce targeted repeat contractions using either small molecules that specifically bind to slipped strand intermediates (Nakamori et al. 2020) or sequence-specific endonucleases to generate DSBs at the repeat locus (Cinesi et al. 2016) were successful in experimental systems with CAG/CTG repeats. It is unclear whether these strategies would apply generally to all diseasecausing DNA repeat sequences or whether the underlying mechanisms of large-scale contractions for different repeats are also distinct. Specifically, we designate the descriptors massive or large scale as the number of repeats that would result in a decrease from symptomatic to unaffected lengths (such as a deletion in >45 repeats for DM2 as opposed to loss of just a few repeats).

In contrast to CAG/CTG repeats, much less is known about the mechanisms of CCTG and reverse complementary CAGG repeat instability. This is a pressing question since individuals with DM2 can have 75-11,000 CCTG repeats in CNBP with an estimated average of 5,000 repeats (Liquori et al. 2001). DM2 is also the only repeat expansion disease currently known to be caused by tetranucleotide repeats. In vitro studies with chemical and enzymatic probing showed that CAGG repeats form stable hairpin structures with a specific base-pairing propensity, which was not prominent for the CCTG orientation (Dere et al. 2004). CAGG/CCTG repeats were also shown to form slipped-strand structures through denaturation and reduplexing experiments (Edwards, Sirito, et al. 2009). In addition, NMR analysis indicated that CCTG repeats form hairpin and dumbbell structures that are much more fluid and dynamic (Lam et al. 2011), displaying an ability to change between different conformations and shift along the DNA duplex. This fluidity is proposed to increase the likelihood that CCTG repeats could escape DNA repair (Guo and Lam 2016a; Guo and Lam 2016b).

Previous studies investigating CAGG/CCTG repeat instability in vivo have relied on plasmid-based systems using Escherichia coli and COS-7 mammalian cell culture (Dere et al. 2004; Dere and Wells 2006). The frequency of expansions and contractions increased with longer starting lengths, and the orientation with CAGG repeats on the leading strand template showed greater instability. Another plasmid study using E. coli found that instability was not dependent on repeat orientation (Edwards, Hashem, et al. 2009).

In the current study, we developed a yeast experimental system to investigate the instability of CAGG/CCTG repeats within a chromosomal context. This system offers an additional advantage of enabling the selection of repeat contractions that exceed 80 repeats in length, for example, from (CCTG)<sub>100</sub> to (CCTG)<sub>20</sub>. Through genetic analysis, we found that HR is involved in large-scale CCTG repeat contractions. We also demonstrate that CAGG/CCTG repeats elevate the rate of DSB formation using a genetic assay for chromosomal arm loss. Altogether, genes that have been well-characterized to control CAG/CTG repeat instability do not affect CAGG/CCTG repeats in the same manner, indicating that the precise genetic control of DNA repeat instability is unique to the specific microsatellite sequence.

# Materials and methods CAGG/CCTG plasmid cloning

PCR was used to amplify a double-stranded product using oligonucleotides with complementary CCTG and CAGG repeats that anneal at their 3' ends. JK178 has a 5' NcoI site followed by CCTG repeats, and JK179 has a 5' SphI site followed by CAGG repeats (Supplementary Table 1). The amplified product was digested with NcoI and SphI and then cloned into the plasmid

designated pYes3-G4G1C1-T150-GAA100 that was digested with the same enzymes (Shah et al. 2014). A plasmid containing (CCTG)<sub>27</sub> was verified by Sanger sequencing. Long CCTG repeats were cloned using CCTG and CAGG oligonucleotides designed with 5' nonpalindromic restriction sites, following a previously described strategy to clone TNRs (Grabczyk and Usdin 1999; Krasilnikova and Mirkin 2004). The repeat tract was amplified from this plasmid using JK188 and JK189, which contain nonpalindromic BsgI sites at their 5' ends (Supplementary Fig. 1). The PCR product was purified and digested with BsgI (NEB R0559). The (CCTG)n/(CAGG)n repeats are positioned between the 2 inverted BsgI sites in such a way that pure repeats with complementary 3' TG and CA overhangs are generated upon digestion with BsgI. The digested DNA was purified again and set up in a ligation reaction (NEB M0202). These fragments will ligate in the head-to-tail direction only. The ligated products were separated on an agarose gel, excised, purified, and blunt-ended with T4 DNA polymerase and Klenow fragment. This fragment was cloned into the plasmid backbone described as (GAA)<sub>0</sub> (Shah et al. 2012), which had been blunt-cut with NaeI and treated with alkaline phosphatase. The plasmid was confirmed to have uninterrupted (CCTG)<sub>100</sub> repeats by Sanger sequencing (Genewiz). The (CCTG)<sub>100</sub> plasmid is designated p18 and contains an overall intron length of 1,047 bp.

A (CCTG)<sub>100</sub> plasmid with a shorter overall intron length (820 bp) was obtained by cutting p18 with blunt end restriction enzymes BsaBI and MscI to remove 227 bp of nonrepetitive sequence. The (CAGG)<sub>100</sub> reverse orientation was obtained through molecular cloning whereby PCR using primers JK354 and JK355 with the p18 template will reverse the position of the XhoI and NotI sites flanking the repeats. The digested fragment was then cloned into p18 that had also been digested with XhoI and NotI.

#### Yeast strain construction for large-scale contractions

All strains are isogenic to Saccharomyces cerevisiae wild-type (WT) strain CH1585 (MATa, leu2-41, trp1-463, ura3-52, and his3-200), an S288C-derived haploid strain used in previous DNA repeat instability studies (ATCC 96098). The reporter cassette was excised from each plasmid using SwaI. Transformants were selected on synthetic complete media lacking tryptophan. The cassette is positioned ~1-kb downstream of ARS306, replacing SGD coordinates 75594-75641 on chromosome III. Correct integration was verified by PCR. The integrity of CCTG repeat length was verified by PCR and Sanger sequencing (Retrogen), and this starting strain is designated YJK168 (Supplementary Table 2).

Except as noted below, gene knockouts and point mutations were constructed using a CRISPR approach with the bRA89 (HPH) or bRA90 plasmid (LEU2) (Anand et al. 2017). The repair template for knockouts was oligonucleotides consisting of the first 45 nucleotides of the open reading frame followed by the last 45 nucleotides (Supplementary Table 3). PCR using primers flanking the disrupted region was used to verify the knockout strains, and additional primers (i.e. JK213/214 or JK402/403) were used to confirm that the repeat length had been maintained. For separation-of-function mutants, the 90-bp repair template included both the gRNA target, introducing a silent mutation into the NGG sequence, as well as the specific separation-of-function mutation. Specific mutations were verified by Sanger sequencing (Retrogen). The Rad52-Y33A allele is referred to as Y66A in its initial description (Mortensen et al. 2002) according to the primary sequence initially published (Adzuma et al. 1984). The first 33 amino acids in the originally published sequence are not included in the protein as the third start codon in the sequence is the one used. For successful transformants, loss of the CRISPR plasmid was verified via plating to ensure that the Cas9 endonuclease is no longer expressed (i.e. sensitivity to

The pol32 $\Delta$ , rad59 $\Delta$ , sae2 $\Delta$ , mre11 $\Delta$ , rmi1 $\Delta$ , and exo1 $\Delta$  strains were constructed using a PCR-based method for direct gene replacement with pAG32 (HphMX4) (Goldstein and McCusker 1999) used as a template for PCR. Correct targeting was verified by PCR with primers flanking the replacement locus and within the HphMX4 cassette.

#### Fluctuation analysis to determine large-scale contraction rates

All strains were initially grown as single colonies on rich media (YPD) agar plates supplemented with 50-µg/mL uracil (referred to as DU) for 72 h at 30°C. Whole, individual colonies were suspended in 1000-μL sterile water. To select for URA+ clones, 100 μL of the cell suspension was directly plated on synthetic complete media lacking uracil (SC-URA), which is composed of 2% glucose, 0.67% yeast nitrogen base, 0.2% drop-out mix synthetic minus uracil (US Biological D9536), and 2% agar. The cell suspension was serially diluted to plate on YPD media (100  $\mu$ L of 10<sup>-5</sup> dilution) for determination of total cell number. For each experiment, at least 12 independent colonies were analyzed, including 2 independent isolates of each strain/genotype. Colonies growing on DU that had an initial contraction or expansion, assessed via repeat length PCR, were excluded from the analysis. All colonies on SC-URA and YPD were counted at 72 h. Rates and 95% CIs were calculated using the Ma-Sandri-Sarkar maximum likelihood estimator (MSS-MLE) method with correction for plating efficiency determined as  $z - 1/z \ln(z)$ , where z is the fraction of the culture analyzed (Rosche and Foster 2000). The average number of viable cells grown on YPD (Nt) was used in all calculations. The web-hosted program FluCalc was used to perform this rate analysis (Radchenko et al. 2018). Large-scale contraction rates were considered to be significantly different if 95% CIs for the rate values did not overlap (Foster 2006).

# Single colony PCR to determine repeat length and generate products for sequencing

Genomic DNA was isolated from single colonies using a previously described method (Aksenova et al. 2013). Cells were resuspended in 1.5 µL of 0.5 mg/mL lyticase solution [0.9 M sorbitol, 0.1 M EDTA (pH 7.4)], incubated at 37°C for 15 min, and then resuspended in  $50\,\mu L$  of water. Samples were incubated at  $100^{\circ}C$  for 5 min and centrifuged at 2,500  $\times$  g for at least 2 min. For PCR analysis of CCTG/CAGG repeat length using primers JK402 and JK403 (441-bp product for (CCTG)<sub>100</sub>), reactions included 1X GC buffer (F519, Thermo Fisher Scientific), 0.2 mM dNTP mix, 0.8  $\mu$ M of each primer, 3% DMSO, 0.4 units of Phusion Hot Start II DNA polymerase (F549, Thermo Fisher Scientific), and  $1.5\,\mu L$  of the DNA supernatant in a 20-μL total reaction volume. Thermocycling conditions were 30 s at 98°C, followed by 32 cycles of 10 s at 98°C, 20 s at 60°C, and 30 s at 72°C, concluding with 10 min at 72°C.

For PCR analysis of CCTG/CAGG repeat length using primers JK213 and JK214 (590-bp product for (CCTG)<sub>100</sub>), reactions included 1X Green GoTaq reaction buffer (M7911, Promega), 0.2 mM dNTP mix, 0.8 µM of each primer, 3% DMSO, 1 unit of Taq (Thermo Fisher Scientific EP0402), and 1.5 μL of the DNA supernatant in a 20-μL total reaction volume. Thermocycling conditions were 60 s at 95°C, followed by 32 cycles of 30 s at 95°C, 20 s at 60°C, and 60 s at 72°C, concluding with 10 min at 72°C.

For PCR analysis of contracted clones (JK15 and JK18) and nonrepetitive DNA (miscellaneous), reactions included 1X Green GoTaq reaction buffer (M7911, Promega), 0.16 mM dNTP mix, 0.8 µM of each primer, 0.5 units of Taq DNA polymerase, and 1.5  $\mu$ L of the DNA supernatant in a 12.5- $\mu$ L total reaction volume. PCR products were cleaned using column-based purification prior to Sanger sequencing.

### Spot assays to characterize yeast growth phenotype

Cells were inoculated from fresh YPEG patches into 5 mL of YPD liquid and grown at 30°C overnight. The culture was then reset to an OD<sub>600</sub> of 0.5, from which five 5-fold serial dilutions were made (i.e.  $5^{-5}$  dilution). From these dilutions, 3  $\mu$ L was plated on rich media (YPD) plates and 5 μL on selective [5-fluoroorotic acid (5-FOA) and SC-URA] plates. The plates were then incubated at 30°C for 72 h, and images were taken at 48 and 72 h.

#### RNA isolation and RT-qPCR analysis

RNA was isolated from log phase cells grown in YPD liquid at 30°C using the YeaStar RNA Kit (Zymo Research R1002) according to manufacturer protocol. Genomic DNA was digested using the TURBO DNA-free kit (Invitrogen AM1907). Complementary DNA (cDNA) was synthesized using 0.5-µg total RNA as template, ProtoScript II Reverse Transcriptase (NEB M0368), and equal amounts of random hexamer primers (Thermo Fisher SO142) and oligo(dT) primers (Thermo Fisher SO131). The cDNA abundance of each strain was quantified using SYBR Green-based qPCR (Thermo Fisher PowerUp A25742) and primers to amplify spliced and unspliced URA3 transcripts, previously described in Shishkin et al. (2009). The delta-delta CT method of relative quantification was used to calculate the relative expression of each region (primer set) compared to the ACT1 gene as an endogenous control. The relative expression in the long intron strain was set to 1 for comparison. At least 3 biological replicates of cDNA for each strain were used for the analysis. The mean relative expression values and SE are plotted.

#### Yeast strain construction for analysis of DNA fragility

Strains to analyze chromosome arm loss were constructed as described (Kim et al. 2008). A DNA fragment containing (CCTG/ CAGG)<sub>100</sub> was generated by PCR using p18 plasmid (described above) as template DNA and primer sets with 5' homology to LYS2. JK510/511 and JK512/513 primer sets would result in opposite repeat orientations with respect to LYS2 (Supplementary Table 4). PCR products were purified by gel extraction and transformed independently into KT119 and KT120 (MATa, his7-2, leu2-3,112, trp1-Δ, ura3-Δ, lys2-Δ, ade2-Δ,bar1-Δ, sfa1-Δ, cup1-1-Δ, yhr054c-4, cup1-2-4, lys2::kanMX-URA3, ADE2, CUP1, and SFA1), as they contained reporter genes relevant to the GCR assay (CAN1 at the endogenous locus on ChrV and ADE2 relocated to ChrV as in Fig. 4) as well as selectable markers for transformant screening (URA3 and KanMX). Replacement of the "core" sequence disrupting LYS2 would result in 5-FOA<sup>R</sup> and G418<sup>S</sup> yeast cells. In addition, we cotransformed the starting strains with a CRISPR plasmid that would direct a DSB at KanMX to increase the likelihood of successful targeting. These transformant clones were analyzed for repeat length by PCR using primers JK514 and JK515 (PCR conditions below) and Sanger sequencing (Genewiz). YJK302-3 is a spontaneous expansion that was verified by sequencing to be (CAGG)<sub>138</sub>.

For PCR analysis of CCTG/CAGG repeat length in GCR strains using primers JK514 and JK515 (655-bp product for (CCTG)<sub>100</sub>), reactions included 1x Green GoTaq reaction buffer (M7911, Promega), 0.2 mM dNTP mix, 0.8 µM of each primer, 3% DMSO, 0.75 units of Taq (Thermo Scientific EP0402), 0.3 units of Phusion Hot Start II DNA polymerase (F549, Thermo Fisher Scientific), and  $1.5 \,\mu L$  of the DNA supernatant in a 20- $\mu L$  total reaction volume. Thermocycling conditions were 60 s at 95°C, followed by 32 cycles of 30 s at 95°C, 20 s at 60°C, and 60 s at 72°C, concluding with 10 min at 72°C.

#### Measurement of chromosome arm loss rates

Rates of chromosome arm loss were determined through fluctuation assays. HMK1/2 strains containing (GAA)<sub>5</sub> repeat tracts served as a negative, nonfragile control. Verified strains were initially grown on YPEG to select against petite mutants. Single colonies were grown on rich media (YPD) plates supplemented with 50-µg/mL uracil (referred to as DU) for 72 h at 30°C. Whole, individual colonies were suspended in 200-µL sterile water. To select for Can<sup>R</sup>Ade – clones, 100 μL of the cell suspension was plated on synthetic media with low adenine (5 µg/mL) and 60-µg/mL canavanine (Sigma C9758) with 2% glucose, 0.67% yeast nitrogen base, and 2% agar. The cell suspension was serially diluted to plate on YPD media (100  $\mu$ L of  $10^{-5}$  dilution) for determination of total cell number. For each independent experiment, at least 12 independent colonies were analyzed. Colonies growing on DU that had an initial contraction or expansion, assessed via repeat length PCR, were excluded from the analysis.

Cells were incubated at 30°C and grown for 7 days. Colony counts occurred on days 3, 5, and/or 7. The same trends were observed on each day, so the data for day 3 colony counts were used to determine rates. Rates and 95% CIs were calculated using the MSS-MLE method as described above for large-scale contractions. Because of the larger 95% CIs associated with these arm loss rates  $(\sim 10^{-8})$ , the average of 3 independent experiments was used to calculate a mean arm loss rate and SE. An unpaired t-test was used to determine statistical significance compared to the control (GAA)<sub>5</sub> strain (HMK1/2).

The same method was used to determine CAN1 mutation rate except that the number of canavanine resistant, white clones (Ade+) was used for fluctuation analysis.

#### Results

#### A system to investigate CAGG/CCTG repeat contractions

To investigate CAGG/CCTG repeat instability, we employed a system previously used to study large-scale GAA repeat expansions (Shishkin et al. 2009) and contractions (Khristich et al. 2020), which are responsible for Friedreich's ataxia (FA). The yeast system mimics the intron location of GAA repeats in the gene responsible for FA, wherein URA3 under the control of its native promoter is artificially split by an intron containing (GAA)<sub>100</sub> repeats and used for forward selection. Large-scale GAA expansions increase the intron length beyond the yeast splicing threshold of ~1 kb (Yu and Gabriel 1999), which impairs URA3 splicing and renders cells resistant to the drug 5-fluoroorotic acid (5-FOA). Cells can also become 5-FOAR through spontaneous point mutations, insertions and deletions, or other mechanisms that inactivate URA3 expression. We adapted the system by cloning (CCTG)<sub>100</sub> repeats into the artificial intron of URA3 (Fig. 1a). The cassette was integrated into chromosome III, ~1 kb away from ARS306, a replication origin that is efficient and activated early in the S phase. In these cells, CCTG is on the sense strand, as it is for CNBP, and lagging strand template for DNA replication. We also constructed an equivalent yeast strain with (CAGG)<sub>100</sub> on the lagging strand template to investigate the effect of repeat orientation.

Unexpectedly, we found that the 2 orientations led to distinct growth phenotypes with respect to uracil auxotrophy (Fig. 1b), despite the total intron length of both strains being identical (1,047 bp). The (CAGG)<sub>100</sub> orientation resulted in a Ura+ phenotype equivalent to URA3 with no intron: growth occurred on synthetic media lacking uracil, whereas no growth occurred on 5-FOA media. In contrast, the (CCTG)<sub>100</sub> orientation showed a predominantly Ura-phenotype with some distinct Ura+ papillae. To exclude the possibility that the (CCTG)<sub>100</sub> strain was Ura – because the intron length exceeded the yeast splicing threshold, we generated yeast with (CCTG)<sub>100</sub> but a shorter overall intron length (820 bp). The growth phenotype was still Ura- in this modified strain (Fig. 1b), though there was greater resistance to 5-FOA than for the longer intron strain. Since the Uraphenotype was dependent on the presence of CCTG repeats rather than exclusively intron length, we used the (CCTG)<sub>100</sub> strain with the 1,047-bp intron length for subsequent analyses of the CCTG orientation to maintain direct comparison to the (CAGG)<sub>100</sub> strain.

We hypothesized that the (CCTG)<sub>100</sub> orientation inhibited functional URA3 expression and that Ura+ clones in the spot assay were due to spontaneous repeat contractions that restored its expression. We performed RT-qPCR to evaluate how transcript levels corresponded to uracil auxotrophy. We observed that a strain with no intron showed >100-fold increase in URA3 transcript abundance compared to the no-repeat intron (971 bp) and (CCTG)<sub>100</sub> strains (Fig. 2). The (CCTG)<sub>100</sub> strain showed a decrease (2.6-fold) in spliced URA3 transcript compared to the no-repeat intron strain, providing evidence that a splicing defect in the CCTG orientation contributes to its Ura- phenotype. In contrast, the (CAGG)<sub>100</sub> strain showed a 3.8-fold increase in spliced URA3 transcript compared to the no-repeat intron strain. This difference in URA3 expression between the 2 orientations was unexpected and is further described in the Discussion.

The difference in gene expression between CAGG and CCTG orientations also restricted what type of instability events, in theory, could be analyzed through selection. For example, since the (CAGG)<sub>100</sub> strain is Ura+ and 5-FOA<sup>S</sup>, we hypothesized that some 5-FOA<sup>R</sup> clones might arise from large-scale CCTG expansions that cause the intron length to exceed the splicing threshold. We determined the rate of 5-FOA resistance (per cell per division) for the (CAGG)<sub>100</sub> strain to be  $5 \times 10^{-7}$  (Supplementary Fig. 2). However, upon PCR analysis of 5-FOAR clones, fewer than 10% showed larger PCR products (Supplementary Fig. 2), indicating that the system needs to be fine-tuned to investigate (CAGG)<sub>100</sub> large-scale expansions in a robust manner. Thus, we focused on the (CCTG)<sub>100</sub> strain and whether cells that changed from Urato Ura+ could be evaluated to study large-scale contractions.

To measure the rate of Ura+ clone formation, we conducted fluctuation tests on the (CCTG)<sub>100</sub> orientation strain. After performing PCR analysis on 24 Ura+ clones using primers flanking the repeats and sequencing the PCR products, we found that the remaining number of repeats ranged from 3 to 15, with a median of 9 repeats (Fig. 1c). This indicates a massive net contraction of over 80 repeats. We calculated the rate of Ura+ clone formation to be  $6 \times 10^{-6}$  per replication (Fig. 1d), which we designate as the WT rate of large-scale contraction based on the PCR and sequencing analyses. To confirm that Ura+clones were not due to gene conversion events with the endogenous ura3-52 allele on chromosome V, which contains a Ty1 retrotransposon insertion, we integrated the (CCTG)<sub>100</sub> cassette into an isogenic background with a full URA3 deletion. We observed an equivalent rate of Ura+ clone formation (Fig. 1d), indicating that they are primarily (if not exclusively) due to large-scale contractions. Next, we focused on delineating the genetic control of large-scale (CCTG)<sub>100</sub> contractions.

#### Impairment of lagging strand synthesis does not affect large-scale CCTG repeat contractions

The previous study investigating large-scale contractions of GAA repeats found that contractions occur during DNA replication rather than DNA repair pathways (Khristich et al. 2020). The median contraction size was ~60 repeat units, and a mechanism involving the bypass of a transient triplex DNA structure during lagging strand synthesis was proposed. Notably, there was a >40-fold increase in large-scale GAA contractions following the loss of Rad27, a 5' to 3' exonuclease and 5' flap endonuclease that processes single-stranded flaps during Okazaki fragment maturation. In contrast, we found that large-scale CCTG contraction rate in the rad27∆ strain was indistinguishable from WT (Fig. 3; Supplementary Table 5). Furthermore, we found only a small increase (1.6-fold) by knocking out the processivity unit of DNA polymerase  $\delta$  (pol324). Because these key proteins in DNA replication and lagging strand DNA synthesis showed no effect on large-scale CCTG contractions, we focused our subsequent genetic analysis on DNA repair pathways.

#### HR is involved in large-scale CCTG repeat contractions

Various DNA repeats have been shown to elevate HR in plasmidbased systems, resulting in expansions and contractions. For example, using an E. coli intramolecular plasmid system, CAGG/ CCTG repeats increased recombination crossover frequencies with expansions being more prevalent than contractions (Dere and Wells 2006). Similar results were observed for CAG/CTG (Napierala et al. 2002) and GAA/TTC (Napierala et al. 2004) repeats using this E. coli system, though contractions were more prevalent. The role of HR on chromosomal DNA repeats is more varied depending on tract length and microsatellite sequence. Loss of Rad51 recombinase and Rad52, which facilitates Rad51 loading, had no effect on short tracts of (CAG)<sub>13</sub> or (CAG)<sub>25</sub> repeats (Miret et al. 1998; Bhattacharyya and Lahue 2004) whereas it did enhance small-scale expansions (Sundararajan et al. 2010) and contractions (Su et al. 2015) of (CAG)70, indicating a protective effect of HR. In contrast, large-scale expansions of (CAG)<sub>140</sub> were dependent on HR through a proposed break-induced replication mechanism (Kim et al. 2017). However, the loss of Rad52 had no effect on large-scale GAA repeat expansions (Shishkin et al. 2009) and a mildly protective effect (2-fold increase in rad524) on large-scale GAA contractions (Khristich et al. 2020).

We observed a 2.2-fold decrease in large-scale contraction rates in rad51\(\delta\) and a 2.3-fold decrease in rad52\(\delta\) compared to WT (Fig. 3), demonstrating that HR promotes this process. We found that this decrease was consistent using 2 analytical methods: nonoverlapping 95% CIs and comparison of multiple trials encompassing 59 independent cultures (Supplementary Fig. 3). Furthermore, we tested whether Rad51 and Rad52 might have a compensatory effect or overlapping functions. The rad5111 rad52∆ double mutant showed a comparable, epistatic (and not synergistic) 1.6-fold decrease to the single mutants, indicating that their roles are in the same genetic pathway. We tested specific mutants to investigate the roles of these proteins further. Rad51-Y388H is defective in interactions with Rad52 as well as Srs2 helicase (Seong et al. 2009). This mutant demonstrated a 1.7-fold decrease in large-scale contraction rate. Rad52-Y33A is defective in DSB repair, as demonstrated by sensitivity to  $\gamma$ -irradiation, but proficient in spontaneous mitotic recombination such as heteroallelic recombination. The large-scale contraction rate of Rad52-Y33A was indistinguishable from WT. We further

evaluated the role of the Rad52 homolog Rad59, which is required for single-strand annealing, and found no difference in large-scale contraction rate compared to WT.

#### Srs2 helicase is not required for large-scale CCTG repeat contractions in unchallenged cells

Srs2 is a DNA helicase that functions in many aspects of DNA replication, repair, and recombination. Notably for DNA repeat instability, Srs2 can unwind CAG, CTG, and CGG substrates in vitro (Bhattacharyya and Lahue 2005). 2D gel-electrophoretic analysis of replication intermediates demonstrated that Srs2 is required in vivo for replication fork progression through these TNRs (Kerrest et al. 2009). Loss of Srs2 function caused an increase in small-scale expansions of (CAG)<sub>25</sub>, (CTG)<sub>25</sub>, and (CGG)<sub>25</sub> repeats (Bhattacharyya and Lahue 2004) and nonselective expansions and contractions of (CTG)<sub>55</sub> (Kerrest et al. 2009), though it had no effect on large-scale expansions of (CAG)<sub>140</sub> (Kim et al. 2017). Because CCTG/CAGG repeats can also form hairpin structures, we investigated loss of Srs2 function in our assay, predicting that there would be an increase in large-scale contractions if Srs2 unwound CCTG/CAGG repeats due to replication bypass of structures formed on the template strand. We found that the rate of large-scale CCTG contractions in srs21 did not differ from WT (Fig. 3).

Because Srs2 has an anti-recombinase role and displaces Rad51 filaments during HR, we tested whether loss of Srs2 function would influence large-scale CCTG contractions when cells were challenged with replication stress, specifically DSBs. When srs24 cells were treated with camptothecin (CPT), a topoisomerase I inhibitor that results in breaks during DNA replication, rates of large-scale CCTG contractions increased over a range of concentrations (Supplementary Fig. 4; Supplementary Table 6). For example, comparing srs24 to WT, there was a 4.8-fold increase at  $10\,\mu M$  CPT and a 5.7-fold increase at  $50\,\mu M$  CPT. In addition, 50 μM CPT increased the contraction rate of srs2Δ cells 11.8-fold compared to untreated srs24 cells, revealing a dose-dependent effect of DNA damage on the role of Srs2 function in large-scale CCTG contractions. Furthermore, we observed a similar increase in contraction rates with hydroxyurea (HU) treatment (Supplementary Fig. 4; Supplementary Table 6), which causes replication fork stalling and uncoupling of the replication fork polymerases and helicase that can result in DSBs. At 50 mM HU, srs21 showed a 3.1-fold increase compared to WT. For both CPT and HU treatments, there was also a ~2-fold increase in contraction rate at all doses in the WT strain compared to no treatment. We propose that the increase is indicative of DSBs that are instigated during the S phase and aberrantly repaired to generate large repeat contractions (see Discussion).

## Sgs1 helicase is required for large-scale CCTG repeat contractions

The RecQ helicase, Sgs1, plays various roles in DNA repair and recombination in budding yeast (Gupta and Schmidt 2020). During recombination, Sgs1 plays an early role in long-range resection at a DNA DSB and was shown to be required for heteroduplex rejection during single-strand annealing (Sugawara et al. 2004). Through biochemical assays, purified Sgs1 was demonstrated to unwind a broad range of DNA structures including Holliday junctions (Cejka and Kowalczykowski 2010) and G-quadruplexes (Huber et al. 2002). Long (CTG)<sub>75</sub> repeats were shown to be stabilized by Sgs1, as loss of function led to increased expansions and contractions under nonselective conditions (Kerrest et al. 2009).

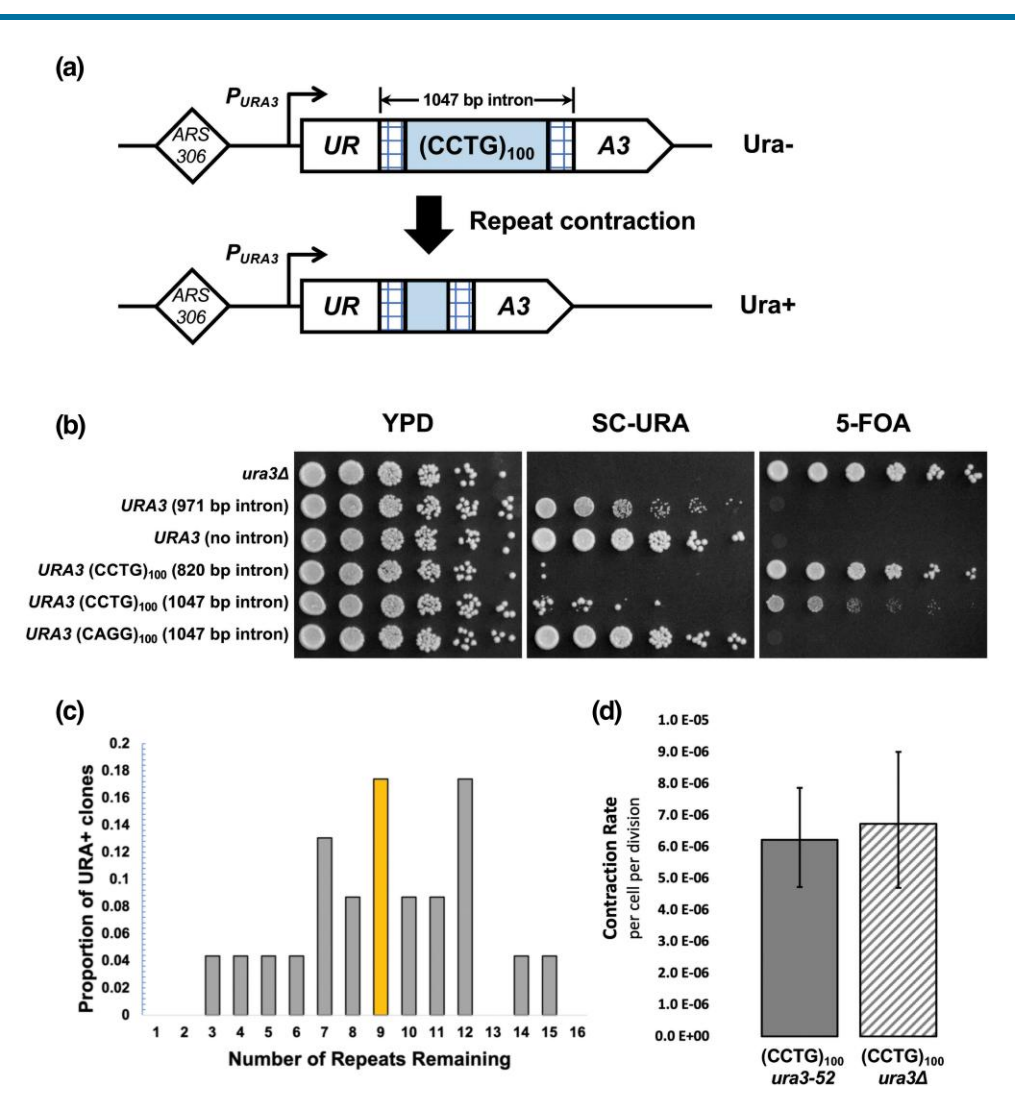


**Fig. 1.** Experimental system to study large-scale CCTG repeat contractions in vivo. a) DNA repeats are cloned into the artificial intron, derived from ACT1, of a URA3 reporter gene. The reporter gene is integrated  $\sim$ 1-kb downstream of the replication origin ARS306. The starting strain with (CCTG)<sub>100</sub> is Ura—. Repeat contraction renders the cells Ura+. b) Spot assays to evaluate the growth phenotypes of yeast strains with (CCTG)<sub>100</sub> and (CAGG)<sub>100</sub> repeats as well as nonrepetitive DNA. c) Distribution of remaining repeat length in Ura+ clones, evaluated by PCR and Sanger sequencing. The median number of repeats was 9. d) Rate of large-scale contraction for (CCTG)<sub>100</sub> strains, shown with 95% CIs. Rate is calculated using the number of Ura+ clones beginning with 12 independent cultures and the MSS-MLE with a correction for sampling and plating efficiency.

The absence of Sgs1 had a considerable effect on large-scale CCTG contraction rate, as  $sgs1\Delta$  showed a 5.7-fold decrease compared to WT (Fig. 3). Interestingly, Sgs1 is required for large-scale contractions even under unperturbed conditions, which is opposite the effect displayed by Srs2 when treated with replicative stressors. To better understand the role of Sgs1 in repeat contractions, we constructed and analyzed a helicase-defective mutation Sgs1-K706A. This strain also displayed a 5.5-fold decrease in contraction rate compared to WT (Fig. 3), indicating that Sgs1 helicase activity is required for its effect on large-scale CCTG contractions. We evaluated the contraction rate in the  $rad51\Delta$  sgs1 $\Delta$  double mutant and found a 10.8-fold decrease in contraction rate compared to WT (Fig. 3). This was a slight decrease compared to the  $sgs1\Delta$  mutant, though the 95% CIs are overlapping.

Having established a requirement for Sgs1 on large-scale CCTG repeat contractions, we investigated whether its role was through facilitating 5′ DNA end resection, a key processing step to promote DSB repair by HR. The Mre11-Rad50-Xrs2 (MRX) complex localizes to a DSB, upon which the Mre11 nuclease can initiate resection. Sae2 has also been shown to be involved in short-range resection, though both Mre11 and Sae2 have been shown to be dispensable

for the resection of DNA ends overall. Long-range, more processive resection is mediated by Sgs1-Dna2 or Exo1 pathways, which may have redundant roles. We found that single mutants of mre114, sae24, and exo14 each displayed large-scale contraction rates that were not significantly different from WT (Supplementary Fig. 5). Sgs1 interacts with Top3 and Rmi1 to form the STR complex, which enhances DNA end resection and resolves recombination intermediates. We did not observe an effect on large-scale contraction rates in the rmi14 mutant.

Because the nuclease domain of Dna2 is essential, its role in DNA resection could not be evaluated through direct knockout. We tested the <code>dna2-H547A</code> mutant, which is described as nuclease-attenuated, though it maintains ATPase and helicase activity (Lee <code>et al. 2000</code>). We found that the mutant displayed a 12-fold elevated rate, suggesting that <code>Dna2</code> nuclease activity plays a protective role in CCTG repeat contractions (Supplementary Fig. 5).

# MMR proteins are differentially involved in large-scale CCTG repeat contractions

DNA mismatch repair (MMR) is initiated by the MutS $\alpha$  and MutS $\beta$  complexes, formed by the Msh2-Msh6 and Msh2-Msh3

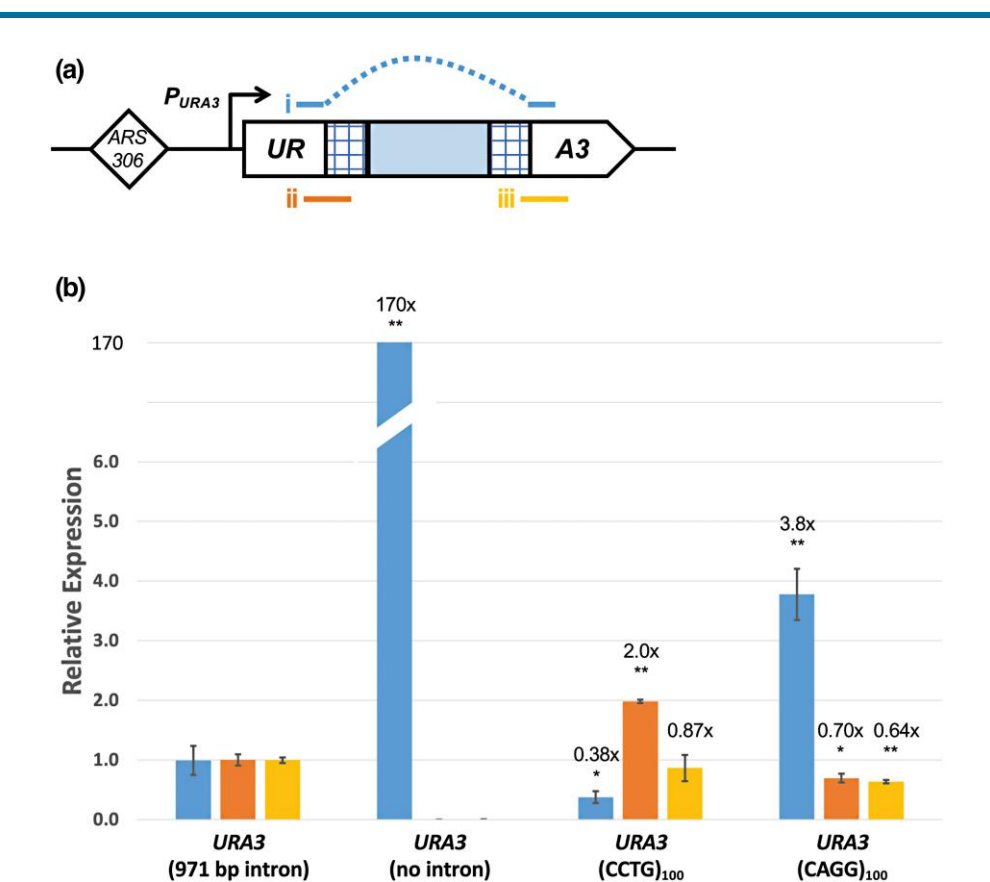


Fig. 2. Comparison of URA3 reporter gene expression in strains with and without CAGG/CCTG repeats. a) Representation of PCR amplicons to evaluate: i) spliced URA3, ii) 5' unspliced URA3, and iii) 3' unspliced URA3. Dashed line denotes that primers will not anneal to the intron sequence. b) Relative expression of spliced and unspliced URA3 transcripts compared to ACT1 endogenous control in 4 yeast strains. Bar graph colors correspond to amplicon colors as in a). The relative expression in the long intron strain was set to 1 for comparison, and the numerical fold difference is in comparison to the long intron strain. At least 3 biological replicates of cDNA for each strain were used for the analysis. The mean relative expression values and SE are plotted. Statistical significance was evaluated by unpaired t-test (\*P < 0.05; \*\*P < 0.01) for each primer set in the no intron, (CCTG)<sub>100</sub>, or (CAGG)<sub>100</sub> cDNA sample compared to the long intron strain.

heterodimers, respectively. MutS $\alpha$  recognizes single-base mismatches, while MutS $\beta$  recognizes insertion/deletion loops. MMR proteins have been implicated in CAG/CTG repeat instability. Specifically, CAG/CTG TNRs were stabilized in the  $msh3\Delta$  mutant (Williams and Surtees 2015). Loss of Msh2 and Msh3, though not Msh6, was shown to decrease expansions in mouse models (Manley et al. 1999; van den Broek et al. 2002; Foiry et al. 2006). These results were corroborated in a human cell culture system (Gannon et al. 2012). However, the loss of MMR proteins had no effect on large-scale (>60 repeats) expansions of CAG/CTG repeat in a yeast experimental system (Kim et al. 2017).

In evaluating large-scale CCTG contractions, we found that loss of MMR proteins demonstrated differential effects (Fig. 3). The strongest effect was displayed by <code>msh34</code>, which showed a 7.0-fold decrease in contraction rate. In contrast, <code>msh24</code> showed no difference and <code>msh64</code> a slight increase (1.6-fold) in contraction rate, both of which were not significant. Following mismatch recognition, proteins in the MutL family function as heterodimers to catalyze repair. They also have roles outside of MMR such as in meiotic recombination (Pannafino and Alani 2021). Large-scale contraction rates in <code>mlh14</code>, <code>mlh24</code>, <code>mlh34</code>, and <code>pms14</code> single mutants were not significantly different from WT.

To evaluate the relationship of Msh3 with Sgs1 and Rad51, we constructed double mutants and tested their effect on large-scale CCTG repeat contractions. The  $sgs1\Delta$  msh3 $\Delta$  mutant showed an 11-fold decrease in contraction rate compared to WT, a slight

decrease compared to the single mutants though the 95% CIs overlap. In contrast, the  $rad51\Delta$  msh3 $\Delta$  mutant showed a rate (2.0-fold decrease) comparable to the  $rad51\Delta$  single mutant, evidence of an epistatic relationship where Rad51 functions upstream of Msh3 in the genetic pathway. We synthesize these genetic results in the Discussion.

# CCTG repeats increase chromosomal fragility in an orientation-dependent manner

To confirm DSB formation caused by CAGG/CCTG repeats, we used a genetic assay (Kim et al. 2008) to determine the rates of chromosomal fragility in both repeat orientations. This assay works by integrating DNA repeats into a relocated lys2 locus on ChrV (Fig. 4a), where DNA breakage can lead to a telomere-proximal deletion (arm loss). This region does not contain essential genes but does contain CAN1 and ADE2. This allows for the selection of canavanine-resistant (Can<sup>R</sup>) and Ade— clones, which appear red, and permits subsequent calculation of DNA fragility rates. For this arm loss assay, we designate repeat orientation as previously described and name the repeat sequence that is on the lagging strand template for DNA replication. This orientation is determined by ARS507, which was characterized by 2D gel analysis of replication intermediates (Zhang et al. 2013).

We tested DNA fragility in  $(CCTG)_{100}$  and  $(CAGG)_{100}$  strains as well as a  $(CAGG)_{138}$  strain that was isolated as a spontaneous expansion during strain construction. We observed an increase in

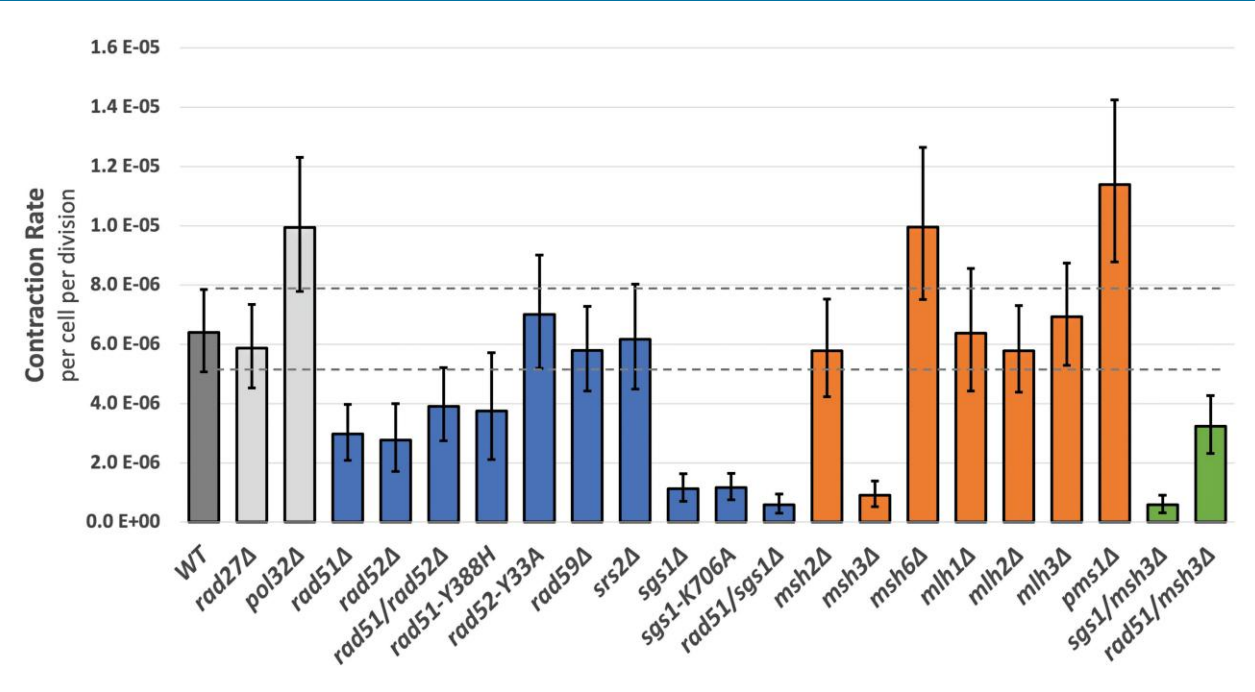


Fig. 3. Genetic analysis of large-scale CCTG repeat contractions. Rate of large-scale contraction for (CCTG)<sub>100</sub> strains, shown with 95% CIs (dashed lines for WT strain). Rate is calculated using the number of Ura+ clones beginning with 12 independent cultures and the MSS-MLE with a correction for sampling and plating efficiency.

Can<sup>R</sup>Ade— clones that was above the background levels of a (GAA)<sub>5</sub> negative control strain but noticeably less than (GAA)<sub>220</sub> (Fig. 4a). Through fluctuation analyses, we quantified arm loss rates of the (CCTG)<sub>100</sub> and (CAGG)<sub>138</sub> orientations to be significantly increased compared to the (GAA)<sub>5</sub> negative control (P < 0.05) whereas (CAGG)<sub>100</sub> showed an upward trend that was not significantly different (Fig. 4c). The rates of CAN1 mutation alone among the CAGG/CCTG strains were not significantly different compared to the (GAA)<sub>5</sub> negative control (Supplementary Fig. 6).

#### **Discussion**

We have established an experimental system to characterize massive contractions of CCTG repeats, showing by genetic analysis that large-scale CCTG contractions occur via HR. Through analysis of double mutants, we characterize epistatic relationships between genes involved in large-scale CCTG contractions. Furthermore, we provide the first evidence that CAGG/CCTG repeats increase DSB formation and chromosomal fragility in vivo.

Large-scale CCTG contractions were not dependent on proteins involved in lagging strand synthesis (Pol32) and Ozakaki fragment processing (Rad27). This demonstrates that the genetic control is distinct from large-scale GAA repeat contractions, which were substantially increased in pol324 and rad274 mutants. However, we did observe an increase in CCTG contractions in the dna2-H547A mutant, which may involve Okazaki fragment processing by cleaving long 5' flaps or another role in DSB end processing (discussed below). GAA repeats form a triplex structure consisting of a GAA/TTC double helix with standard Watson Crick base pairing and, in its most stable configuration, a third GAA homopurine strand that anneals via reverse Hoogsteen hydrogen bonds. Large contractions of GAA repeats were proposed through DNA polymerase occasionally bypassing this secondary structure (Khristich et al. 2020). However, CAGG/CCTG repeats are not predicted to form triplex structures. Rather, there is gel electrophoretic evidence for hairpins (more stable in the CAGG orientation) (Dere et al. 2004) and slipped strand DNA (Edwards, Sirito, et al. 2009). High-resolution NMR studies with nucleotide substitution experiments have illuminated additional secondary structures such as dumbbells, minidumbbells, and loops, which may interchange configurations rapidly. Though strand slippage on the template strand is likely to contribute to some repeat contractions, these are likely to be 1-to-3 unit deletion events.

Since we observe very large CCTG repeat contractions exceeding 80 repeat units, we describe a model for repeat contractions that is distinct from replication slippage (Fig. 5). Both CPT and HU treatments elevate contraction rates even in the WT strain. Thus, we propose that DSBs are generated during the S phase, though indirect effects of the replication stress response are a possibility that remains to be tested. Because of the high GC content and structure-forming potential of the repeats, replication through the repeat tract may result in the uncoupling of the replication fork helicase and polymerase. This uncoupling could increase the persistence of single-stranded DNA (ssDNA) and exacerbate secondary structure formation, structures that could be stabilized by MutS\(\beta\) (Tian et al. 2009; Zhao et al. 2015). A 2-ended DSB could then be generated by structure-specific nucleases acting at the distortion(s) in B-DNA, though the nucleases involved remain to be identified. Next, the DSB is repaired by HR, analogous to a fork restart mechanism. Because of the repetitive nature of the DNA template, out-of-register alignment will result in a massive contraction. Importantly, only events where the invading DNA end aligns toward the edge of the repeat tract on the template strand will result in a large enough repeat contraction for Ura+ selection. We believe such events are more likely due to the hairpin-forming potential in the CAGG orientation. Next, we summarize some of our genetic analysis to describe how Rad51, Rad52, Sgs1, Dna2, and Msh3 may be acting.

Large-scale CCTG contractions were dependent on Rad51 and Rad52, though the effect was modest (a 2-fold decrease in knockouts). In a previous study examining single-strand annealing

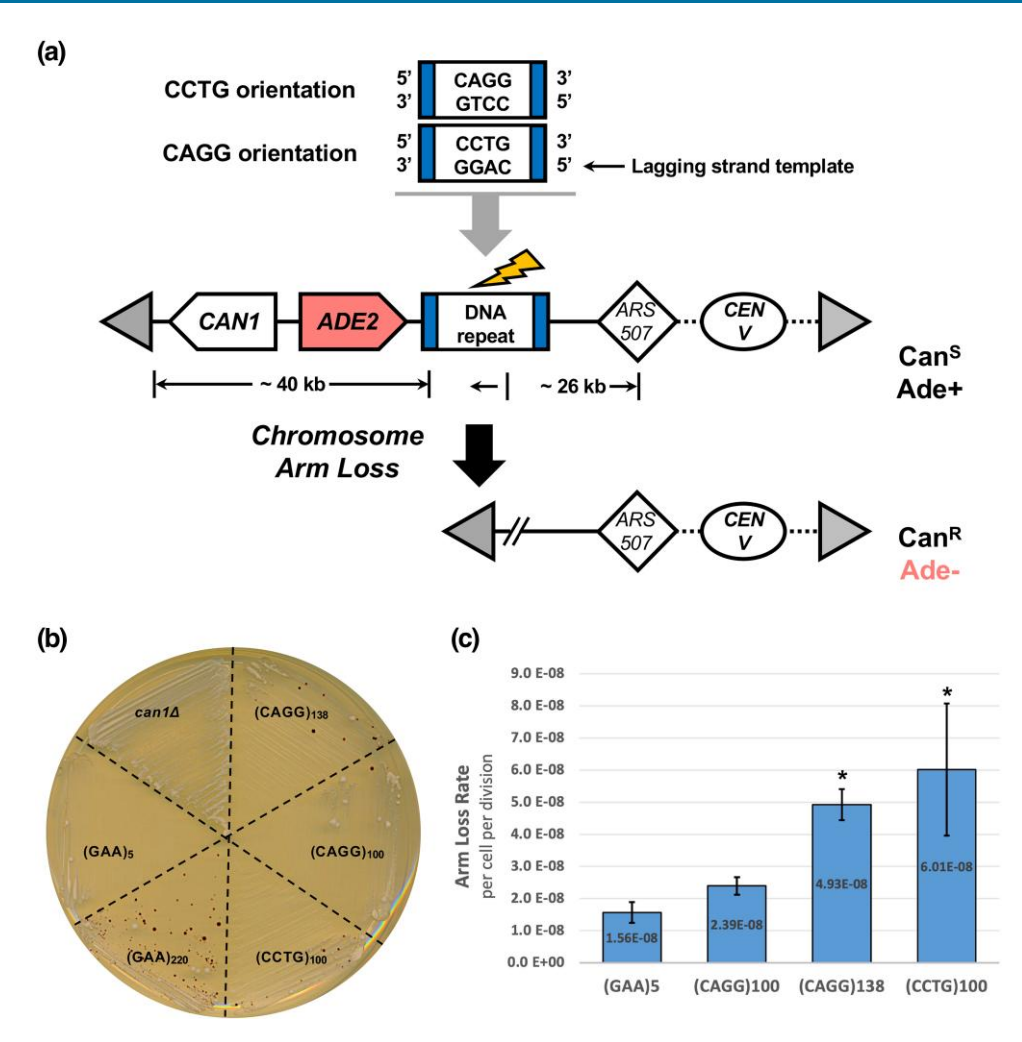


Fig. 4. CCTG repeats elevate chromosomal fragility in an orientation-dependent manner. a) Experimental system to study repeat-induced DNA fragility via chromosomal arm loss. CCTG and CAGG repeats were integrated at the reporter locus, lys2 (blue). DSB formation followed by telomere addition (gray triangle) will result in increased arm loss frequency of the left chromosomal arm. This region (~40 kb) contains no essential genes and the selectable markers CAN1 and ADE2. Mutations in these genes result in canavanine-resistant (Can<sup>R</sup>) and adenine auxotroph clones (Ade-) that appear red when plated on selective media. The closest origin of replication is ARS507. As such, the lagging strand template for DNA replication is noted at the top of the figure. The CCTG and CAGG orientations refer to their placement on the lagging strand template. b) Growth of strains on media containing canavanine and low adenine (5  $\mu$ g/mL). (GAA)<sub>5</sub> and (GAA)<sub>220</sub> strains are described in (41). c) CCTG/CAGG repeats elevate arm loss rates. Arm loss rates of (GAA)<sub>5</sub>, (CAGG)<sub>138</sub>, and (CCTG)100 from 3-day incubation on selective media. Arm loss rates were calculated with FluCalc, which uses the MSS-MLE model with a correction for sampling and plating efficiency. Error bars indicate SE from 3 independent experiments. Statistical significance was evaluated by unpaired t-test (\*P < 0.05) for each CAGG/CCTG strain compared to the nonfragile (GAA)<sub>5</sub> control.

within the ribosomal DNA array, RAD52 was not essential, and it was proposed that the presence of large amounts of homology enabled Rad52-independent DSB repair (Ozenberger and Roeder 1991). The simple tandem repeat nature of the CCTG locus may make Rad51 and Rad52 dispensable for homology search leading to DSB repair. In our double mutant analysis, none of the effects were synergistic. Some double mutants were clearly epistatic ( $rad51\Delta \ rad52\Delta$  and  $rad51\Delta \ msh3\Delta$ ), and others were epistatic or possibly additive ( $rad51\Delta \ sgs1\Delta \ and \ sgs1\Delta \ msh3\Delta$ ). To harmonize these results, we interpret a genetic relationship with Sgs1 upstream of Rad51.

Among its various roles in DNA repair, Sgs1 is known to promote 5′ DNA resection to form a longer 3′ ssDNA tail via its 3′ to 5′ helicase/translocation activity (Cejka and Kowalczykowski 2010). Sgs1 is also proposed to help translocation of the invading strand along a Holliday junction through interaction with Rad51, perhaps facilitating the search for homology. Because homology search at the CCTG repeats may not rely solely on Rad51 and Rad52, as described above, we investigated whether

genes involved in DNA resection would also be required for large-scale CCTG contractions. We did not find an effect by deleting MRE11 (MRX complex), SAE2, RMI1 (STR complex), or EXO1. Thus, there may be redundant exonucleases that, along with Sgs1, generate the 3' overhangs for HR. We tested the dna2-H547A mutant that has been shown to have diminished endonuclease activity but unaffected ATPase and helicase activity (Lee et al. 2000). We found that contractions were increased 7.5-fold in the dna2-H547A mutant, which was the opposite effect in the sgs14 mutant. The role of DNA2, which is essential, remains to be elucidated further. However, because Sgs1 and Dna2 physically interact (Cejka et al. 2010), one possibility is that Dna2 counteracts Sgs1 activity in promoting CCTG contractions. Thus, in the absence of Dna2 endonuclease activity, Sgs1 can unwind the repeat tract more extensively, and subsequent hairpin formation on the newly unwound CAGG strand would then increase the likelihood of strand invasion at the distal edge of the repeat tract (Fig. 5). In contrast, when Dna2 activity is unperturbed, DNA unwinding and strand resection may be more limited since Rad52

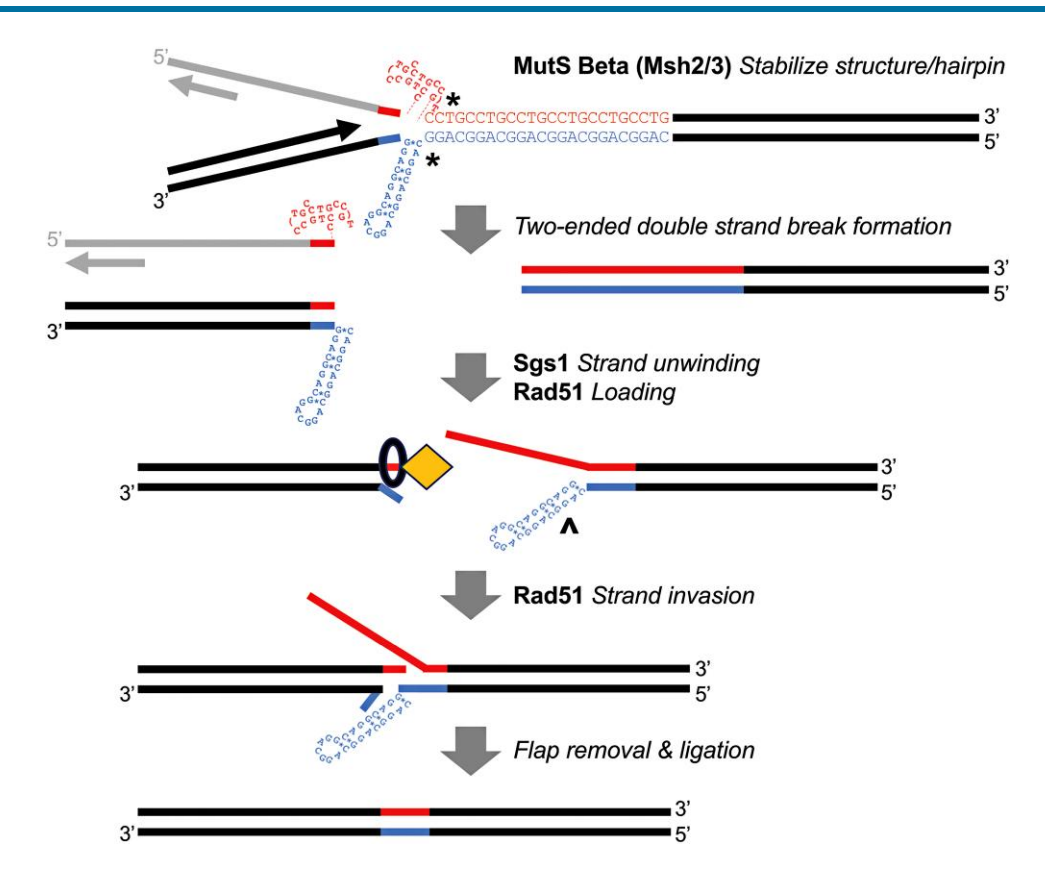


Fig. 5. Proposed model of CCTG repeat contraction in budding yeast. During DNA replication, secondary structures such as dumbbells and hairpins form on ssDNA. ssDNA formation could be elevated due to the uncoupling of DNA polymerases and helicase at the replication fork when replicating through  $the \ DNA \ repeats \ (red/blue \ tracts). \ DNA \ DSBs \ occur \ at \ the \ CAGG/CCTG \ repeats, \ possibly \ mediated \ by \ a \ structure-specific \ nuclease(s). \ Sgs1 \ helicase$ promotes DNA strand unwinding, translocating in a 3' to 5' direction. At the DSB end close to the start of the repeat tract, the 5' end will be displaced by Sgs1 (hairpin omitted for clarity). At the 3' end, Rad52 (black circle) will help load Rad51 (yellow diamond) in a 5' to 3' direction. At the other DSB end in the absence of Dna2 endonuclease activity, Sgs1 can unwind the repeat DNA more extensively. Hairpin formation can occur on the newly displaced CAGG strand (^). Rad51 and Rad52 promote DNA invasion of the CCTG 3' overhang to the homologous template. Because of the repetitive nature of the DNA template, out-of-register alignment toward the distal end of the repeat tract will result in a massive contraction. Importantly, only events where the invading DNA end aligns toward the edge of the repeat tract on the template strand will result in a large enough repeat contraction for Ura+ selection. MutSß may be involved in stabilizing secondary structures and/or processing flap removal following strand annealing.

would be loaded in a 5' to 3' direction from the newly resected end. In this scenario, a single-strand annealing mechanism may contribute to small-scale contractions that are not detected in our selectable system (Supplementary Fig. 7). These models remain to be tested with further single and double mutant analysis.

MMR genes have been widely studied to investigate microsatellite DNA repeat instability, and their described roles depend on various factors including repeat sequence, length, and scale of expansion (Sia et al. 1997). We found that Msh3 is necessary for large-scale CCTG contractions, whereas Msh2 had no effect and Msh6 showed a slightly protective effect. As Msh2/3 forms a heterodimer, it is unclear why the msh24 mutant did not show a concomitant effect as msh34. One possibility is that the Msh2/6 heterodimer plays an opposing role, which was proposed in a previous study investigating CAG/CTG repeat expansions. However, in that study, the absence of a phenotype in msh24 mutants was explained by opposing effects of Msh3 and Msh6 on lagging strand synthesis (Kantartzis et al. 2012), a pathway we did not observe to play a major role in large-scale CCTG contractions. Msh2/3 has been shown to bind insertion/deletion mismatches in yeast (Habraken et al. 1996). Thus, one possibility is that the heterodimer is involved in recognizing the DNA lesion that contributes to the DNA break. However, our double mutant analysis also places RAD51 genetically upstream of MSH3. Thus, Msh3 may also be involved in a later step such as flap removal, like its described role in

single-strand annealing (Sugawara et al. 2004; Bhargava et al. 2016). Characterizing the role of Msh3 warrants further investigation to clarify the role of MMR on large-scale CCTG contractions.

Although the primary focus of this study was to investigate CCTG DNA repeat instability, our results show an intriguing difference of repeat orientation on gene expression. Namely, the (CAGG)<sub>100</sub> orientation showed increased spliced URA3 transcript compared to the (CCTG)<sub>100</sub> orientation, which corresponded to growth on media lacking uracil. Based on the qPCR analysis, we propose that the CCTG orientation impairs the splicing of the CCUG repeat containing RNA since there is a greater abundance of 5'-unspliced URA3 transcript in the (CCTG)<sub>100</sub> orientation. However, other mechanisms remain to be explored such as intron retention, which was demonstrated through transcriptome analysis from DM2 patient samples (Sznajder et al. 2018), or RNA cleavage, which was previously shown with (UUC)<sub>n</sub> RNA in E. coli (Krasilnikova et al. 2007).

Finally, we have shown that disease-causing lengths of CCTG repeats cause chromosomal fragility in vivo. Because the assay requires DSB formation followed by DNA repair via telomere addition or break-induced replication with a nonhomologous template, the rate of arm loss is likely to be an underestimate of total DSB formation induced by CCTG repeats. Given that CCTG repeat length can reach thousands in DM2 patients, it is possible that DSB repair mechanisms might also contribute to such

massive repeat expansions in human cells. Our (CCTG)<sub>100</sub> strain does not permit the selection of large-scale expansions since the starting strain is already Ura-. Thus, new experimental models will need to be developed and fine-tuned to analyze large-scale CCTG repeat expansions in a systematic way. In addition, it was shown that CCTG/CAGG tracts decreased significantly in the affected offspring of DM2 patients (Day et al. 2003), and one intriguing possibility is that such contractions result from recombination following programmed DSBs during meiosis. One bioinformatic study proposed that the DM2 CCTG repeats may have originated from an AluSx element insertion (Kurosaki et al. 2012). As long-read sequencing of repetitive DNA continues to advance, it will be important to evaluate the prevalence of CCTG repeats in the human genome and their molecular properties of expansions, contractions, and DNA fragility.

## Data availability

All data, yeast strains, and plasmids underlying this article will be shared on request to the corresponding author. Supplementary Tables 1, 3, and 4 contain a list of primers used for CCTG/CAGG repeat cloning and RNA analysis, genetic analysis and mutant strain construction, and GCR strain construction, respectively. Supplementary Table 2 contains a list of the strains used.

Supplemental material available at G3 online.

# **Acknowledgments**

We thank Kirill Lobachev for the reagents, James Haber for the CRISPR plasmids, Alexandra Khristich for the advice on mutant construction, and the Mirkin Lab for the helpful discussions. We thank Derrek Schartz and Kara Kolar for the technical assistance during the preliminary stages of this project, Gaby Ramirez for the help with plasmid cloning, and Cedric Lansangan for the strain construction of no-repeat control strains. This paper is dedicated to the memory of Stephen T. Warren, a discoverer of repeat expansions diseases, who succumbed to myotonic muscular dystrophy type 2.

# **Funding**

Research in the Kim Lab is supported by National Institute of General Medical Sciences SC3GM127198 with prior support from K12GM074869. Undergraduate research support was provided by various programs: California State University San Marcos Summer Scholars (DP and AD), National Institutes of Health T34 GM008807 (TH and SH), and National Science Foundation Research Experiences for Undergraduates 1852189 (BA), and National Science Foundation Research Experiences for Undergradutes 1852189 (MO). LH was supported by a California State University Graduate Student Research Restart Award. Research in the Mirkin Lab is supported by the National Institute of General Medical Sciences (R35GM130322) and the National Science Foundation (2153071).

#### **Conflicts of interest**

The authors declare that there is no conflict of interest.

#### Literature cited

Adzuma K, Ogawa T, Ogawa H. 1984. Primary structure of the RAD52 gene in Saccharomyces cerevisiae. Mol Cell Biol. 4(12):2735–2744. doi:10.1128/mcb.4.12.2735-2744.1984.

- Aksenova AY, Greenwell PW, Dominska M, Shishkin AA, Kim JC, Petes TD, Mirkin SM. 2013. Genome rearrangements caused by interstitial telomeric sequences in yeast. Proc Natl Acad Sci U S A. 110(49):19866–19871. doi:10.1073/pnas.1319313110.
- Anand R. Memisoglu G. Haber J. 2017, Cas9-mediated gene editing in Saccharomyces cerevisiae. Protoc Exch. 10.1038/protex.2017.021a.
- Bhargava R, Onyango DO, Stark JM. 2016. Regulation of single-strand annealing and its role in genome maintenance. Trends Genet. 32(9):566-575. doi:10.1016/j.tig.2016.06.007.
- Bhattacharyya S, Lahue RS. 2004. Saccharomyces cerevisiae Srs2 DNA helicase selectively blocks expansions of trinucleotide repeats. Mol Cell Biol. 24(17):7324-7330. doi:10.1128/MCB.24.17.7324-7330.2004.
- Bhattacharyya S, Lahue RS. 2005. Srs2 helicase of Saccharomyces cerevisiae selectively unwinds triplet repeat DNA. J Biol Chem. 280(39):33311-33317. doi:10.1074/jbc.M503325200.
- Callahan JL, Andrews KJ, Zakian VA, Freudenreich CH. 2003. Mutations in yeast replication proteins that increase CAG/CTG expansions also increase repeat fragility. Mol Cell Biol. 23(21): 7849-7860. doi:10.1128/MCB.23.21.7849-7860.2003.
- Cejka P, Cannavo E, Polaczek P, Masuda-Sasa T, Pokharel S, Campbell JL, Kowalczykowski SC. 2010. DNA end resection by Dna2-Sgs1-RPA and its stimulation by Top3-Rmi1 and Mre11-Rad50-Xrs2. Nature. 467(7311):112-116. doi:10.1038/nature09355.
- Cejka P, Kowalczykowski SC. 2010. The full-length Saccharomyces cerevisiae Sgs1 protein is a vigorous DNA helicase that preferentially unwinds Holliday junctions. J Biol Chem. 285(11):8290-8301. doi: 10.1074/jbc.M109.083196.
- Cinesi C, Aeschbach L, Yang B, Dion V. 2016. Contracting CAG/CTG repeats using the CRISPR-Cas9 nickase. Nat Commun. 7(1): 13272. doi:10.1038/ncomms13272.
- Day JW, Ricker K, Jacobsen JF, Rasmussen LJ, Dick KA, Kress W, Schneider C, Koch MC, Beilman GJ, Harrison AR, et al. 2003. Myotonic dystrophy type 2: molecular, diagnostic and clinical spectrum. Neurology. 60(4):657-664. doi:10.1212/01.WNL. 0000054481.84978.F9.
- Dere R, Napierala M, Ranum LP, Wells RD. 2004. Hairpin structureforming propensity of the (CCTG.CAGG) tetranucleotide repeats contributes to the genetic instability associated with myotonic dystrophy type 2. J Biol Chem. 279(40):41715-41726. doi:10.1074/ jbc.M406415200.
- Dere R, Wells RD. 2006. DM2 CCTG\*CAGG repeats are crossover hotspots that are more prone to expansions than the DM1 CTG\*CAG repeats in Escherichia coli. J Mol Biol. 360(1):21-36. doi:10.1016/j. jmb.2006.05.012.
- Edwards SF, Hashem VI, Klysik EA, Sinden RR. 2009. Genetic instabilities of (CCTG).(CAGG) and (ATTCT).(AGAAT) disease-associated repeats reveal multiple pathways for repeat deletion. Mol Carcinog. 48(4):336-349. doi:10.1002/mc.20534.
- Edwards SF, Sirito M, Krahe R, Sinden RR. 2009. A Z-DNA sequence reduces slipped-strand structure formation in the myotonic dystrophy type 2 (CCTG) x (CAGG) repeat. Proc Natl Acad Sci U S A. 106(9):3270-3275. doi:10.1073/pnas.0807699106.
- Foiry L, Dong L, Savouret C, Hubert L, te Riele H, Junien C, Gourdon G. 2006. Msh3 is a limiting factor in the formation of intergenerational CTG expansions in DM1 transgenic mice. Hum Genet. 119(5):520-526. doi:10.1007/s00439-006-0164-7.
- Foster PL. 2006. Methods for determining spontaneous mutation rates. Methods Enzymol. 409:195-213. doi:10.1016/S0076-6879(05)09012-9.
- Fouche N, Ozgur S, Roy D, Griffith JD. 2006. Replication fork regression in repetitive DNAs. Nucleic Acids Res. 34(20):6044-6050. doi:10.1093/nar/gkl757.

- Gannon AM, Frizzell A, Healy E, Lahue RS. 2012. Mutsbeta and histone deacetylase complexes promote expansions of trinucleotide repeats in human cells. Nucleic Acids Res. 40(20):10324-10333. doi:10.1093/nar/gks810.
- Goldstein AL, McCusker JH, 1999. Three new dominant drug resistance cassettes for gene disruption in Saccharomyces cerevisiae. Yeast. 15(14):1541-1553. doi:10.1002/(SICI)1097-0061(199910)15: 14<1541::AID-YEA476>3.0.CO;2-K.
- Grabczyk E, Usdin K. 1999. Generation of microgram quantities of trinucleotide repeat tracts of defined length, interspersion pattern, and orientation. Anal Biochem. 267(1):241-243. doi:10.1006/abio. 1998.2962.
- Guo P, Lam SL. 2016a. Minidumbbell: a new form of native DNA structure. J Am Chem Soc. 138(38):12534-12540. doi:10.1021/ jacs.6b06897.
- Guo P, Lam SL. 2016b. Unusual structures of CCTG repeats and their participation in repeat expansion. Biomol Concepts. 7(5-6): 331-340. doi:10.1515/bmc-2016-0024.
- Gupta SV, Schmidt KH. 2020. Maintenance of yeast genome integrity by RecQ family DNA helicases. Genes (Basel). 11(2):205. doi:10. 3390/genes11020205.
- Habraken Y, Sung P, Prakash L, Prakash S. 1996. Binding of insertion/deletion DNA mismatches by the heterodimer of yeast mismatch repair proteins MSH2 and MSH3. Curr Biol. 6(9):1185-1187. doi:10. 1016/S0960-9822(02)70686-6.
- Huber MD, Lee DC, Maizels N. 2002. G4 DNA unwinding by BLM and Sgs1p: substrate specificity and substrate-specific inhibition. Nucleic Acids Res. 30(18):3954-3961. doi:10.1093/nar/gkf530.
- Izzo M, Battistini J, Provenzano C, Martelli F, Cardinali B, Falcone G. 2022. Molecular therapies for myotonic dystrophy type 1: from small drugs to gene editing. Int J Mol Sci. 23(9):4622. doi:10. 3390/ijms23094622.
- Kantartzis A, Williams GM, Balakrishnan L, Roberts RL, Surtees JA, Bambara RA. 2012. Msh2-Msh3 interferes with Okazaki fragment processing to promote trinucleotide repeat expansions. Cell Rep. 2(2):216-222. doi:10.1016/j.celrep.2012.06.020.
- Kerrest A, Anand RP, Sundararajan R, Bermejo R, Liberi G, Dujon B, Freudenreich CH, Richard G-F. 2009. SRS2 and SGS1 prevent chromosomal breaks and stabilize triplet repeats by restraining recombination. Nat Struct Molec Biol. 16(2):159-167. doi:10. 1038/nsmb.1544.
- Khristich AN, Armenia JF, Matera RM, Kolchinski AA, Mirkin SM. 2020. Large-scale contractions of Friedreich's ataxia GAA repeats in yeast occur during DNA replication due to their triplexforming ability. Proc Natl Acad Sci U S A. 117(3):1628-1637. doi: 10.1073/pnas.1913416117.
- Khristich AN, Mirkin SM. 2020. On the wrong DNA track: molecular mechanisms of repeat-mediated genome instability. J Biol Chem. 295(13):4134-4170. doi:10.1074/jbc.REV119.007678.
- Kim JC, Harris ST, Dinter T, Shah KA, Mirkin SM. 2017. The role of break-induced replication in large-scale expansions of (CAG) n/(CTG)n repeats. Nat Struct Mol Biol. 24(1):55-60. doi:10.1038/ nsmb.3334.
- Kim JC, Mirkin SM. 2013. The balancing act of DNA repeat expansions. Curr Opin Genet Dev. 23(3):280-288. doi:10.1016/j.gde.2013.04.009.
- Kim HM, Narayanan V, Mieczkowski PA, Petes TD, Krasilnikova MM, Mirkin SM, Lobachev KS. 2008. Chromosome fragility at GAA tracts in yeast depends on repeat orientation and requires mismatch repair. EMBO J. 27(21):2896-2906. doi:10.1038/emboj.2008.205.
- Krasilnikova MM, Kireeva ML, Petrovic V, Knijnikova N, Kashlev M, Mirkin SM. 2007. Effects of Friedreich's ataxia (GAA)n\*(TTC)n repeats on RNA synthesis and stability. Nucleic Acids Res. 35(4): 1075-1084. doi:10.1093/nar/gkl1140.

- Krasilnikova MM, Mirkin SM. 2004. Replication stalling at Friedreich's ataxia (GAA)n repeats in vivo. Mol Cell Biol. 24(6):2286-2295. doi: 10.1128/MCB.24.6.2286-2295.2004.
- Kurosaki T, Ueda S, Ishida T, Abe K, Ohno K, Matsuura T. 2012. The unstable CCTG repeat responsible for myotonic dystrophy type 2 originates from an AluSx element insertion into an early primate genome. PLoS One. 7(6):e38379. doi:10.1371/journal.pone. 0038379.
- Lam SL, Wu F, Yang H, Chi LM. 2011. The origin of genetic instability in CCTG repeats. Nucleic Acids Res. 39(14):6260-6268. doi:10. 1093/nar/gkr185.
- Lee KH, Kim DW, Bae SH, Kim JA, Ryu GH, Kwon YN, Kim KA, Koo HS, Seo YS. 2000. The endonuclease activity of the yeast Dna2 enzyme is essential in vivo. Nucleic Acids Res. 28(15):2873-2881. doi:10.1093/nar/28.15.2873.
- Liquori CL, Ricker K, Moseley ML, Jacobsen JF, Kress W, Naylor SL, Day JW, Ranum LPW. 2001. Myotonic dystrophy type 2 caused by a CCTG expansion in intron 1 of ZNF9. Science. 293(5531): 864-867. doi:10.1126/science.1062125.
- Manley K, Shirley TL, Flaherty L, Messer A. 1999. Msh2 deficiency prevents in vivo somatic instability of the CAG repeat in Huntington disease transgenic mice. Nat Genet. 23(4):471-473. doi:10.1038/
- Meola G, Cardani R. 2015. Myotonic dystrophies: an update on clinical aspects, genetic, pathology, and molecular pathomechanisms. Biochim Biophys Acta. 1852(4):594-606. doi:10.1016/j.bbadis. 2014.05.019.
- Miret JJ, Pessoa-Brandao L, Lahue RS. 1998. Orientation-dependent and sequence-specific expansions of CTG/CAG trinucleotide repeats in Saccharomyces cerevisiae. Proc Natl Acad Sci U S A. 95(21):12438-12443. doi:10.1073/pnas.95.21.12438.
- Mortensen UH, Erdeniz N, Feng Q, Rothstein R. 2002. A molecular genetic dissection of the evolutionarily conserved N terminus of yeast Rad52. Genetics. 161(2):549-562. doi:10.1093/genetics/161.
- Nakamori M, Panigrahi GB, Lanni S, Gall-Duncan T, Hayakawa H, Tanaka H, Luo J, Otabe T, Li J, Sakata A, et al. 2020. A slipped-CAG DNA-binding small molecule induces trinucleotide-repeat contractions in vivo. Nat Genet. 52(2): 146-159. doi:10.1038/s41588-019-0575-8.
- Napierala M, Dere R, Vetcher A, Wells RD. 2004. Structure-dependent recombination hot spot activity of GAA.TTC sequences from intron 1 of the Friedreich's ataxia gene. J Biol Chem. 279(8): 6444-6454. doi:10.1074/jbc.M309596200.
- Napierala M, Parniewski P, Pluciennik A, Wells RD. 2002. Long CTG.CAG repeat sequences markedly stimulate intramolecular recombination. J Biol Chem. 277(37):34087-34100. doi:10.1074/ jbc.M202128200.
- Ozenberger BA, Roeder GS. 1991. A unique pathway of double-strand break repair operates in tandemly repeated genes. Mol Cell Biol. 11(3):1222-1231. doi:10.1128/mcb.11.3.1222-1231.1991.
- Pannafino G, Alani E. 2021. Coordinated and independent roles for MLH subunits in DNA repair. Cells. 10(4):948. doi:10.3390/ cells10040948.
- Pearson CE, Sinden RR. 1998. Trinucleotide repeat DNA structures: dynamic mutations from dynamic DNA. Curr Opin Struct Biol. 8(3):321-330. doi:10.1016/S0959-440X(98)80065-1.
- Poggi L, Richard GF. 2021. Alternative DNA structures in vivo: molecular evidence and remaining questions. Microbiol Mol Biol Rev. 85:e00110-20. doi:10.1128/MMBR.00110-20.
- Polleys EJ, Freudenreich CH. 2020. Genetic assays to study repeat fragility in Saccharomyces cerevisiae. Methods Mol Biol. 2056:83–101. doi:10.1007/978-1-4939-9784-8\_5.

- Polleys EJ, Freudenreich CH. 2021. Homologous recombination within repetitive DNA. Curr Opin Genet Dev. 71:143-153. doi:10.1016/j. gde.2021.08.005.
- Polyzos AA, McMurray CT. 2017. Close encounters: moving along bumps, breaks, and bubbles on expanded trinucleotide tracts. DNA Repair (Amst). 56:144–155. doi:10.1016/j.dnarep.2017.06.017.
- Radchenko EA, McGinty RJ, Aksenova AY, Neil AJ, Mirkin SM. 2018. Quantitative analysis of the rates for repeat-mediated genome instability in a yeast experimental system. Methods Mol Biol. 1672:421-438. doi:10.1007/978-1-4939-7306-4 29.
- Rosche WA, Foster PL. 2000. Determining mutation rates in bacterial populations. Methods. 20(1):4-17. doi:10.1006/meth.1999.0901.
- Seong C, Colavito S, Kwon Y, Sung P, Krejci L. 2009. Regulation of Rad51 recombinase presynaptic filament assembly via interactions with the Rad52 mediator and the Srs2 anti-recombinase. J Biol Chem. 284(36):24363-24371. doi:10.1074/jbc.M109.032953.
- Shah KA, McGinty RJ, Egorova VI, Mirkin SM. 2014. Coupling transcriptional state to large-scale repeat expansions in yeast. Cell Rep. 9(5):1594-1602. doi:10.1016/j.celrep.2014.10.048.
- Shah KA, Shishkin AA, Voineagu I, Pavlov YI, Shcherbakova PV, Mirkin SM. 2012. Role of DNA polymerases in repeat-mediated genome instability. Cell Rep. 2(5):1088-1095. doi:10.1016/j. celrep.2012.10.006.
- Shishkin AA, Voineagu I, Matera R, Cherng N, Chernet BT, Krasilnikova MM, Narayanan V, Lobachev KS, Mirkin SM. 2009. Large-scale expansions of Friedreich's ataxia GAA repeats in yeast. Mol Cell. 35(1):82-92. doi:10.1016/j.molcel.2009.06.017.
- Sia EA, Kokoska RJ, Dominska M, Greenwell P, Petes TD. 1997. Microsatellite instability in yeast: dependence on repeat unit size and DNA mismatch repair genes. Mol Cell Biol. 17(5): 2851-2858. doi:10.1128/MCB.17.5.2851.
- Su XA, Dion V, Gasser SM, Freudenreich CH. 2015. Regulation of recombination at yeast nuclear pores controls repair and triplet repeat stability. Genes Dev. 29(10):1006-1017. doi:10.1101/gad. 256404.114.
- Sugawara N, Goldfarb T, Studamire B, Alani E, Haber JE. 2004. Heteroduplex rejection during single-strand annealing requires Sgs1 helicase and mismatch repair proteins Msh2 and Msh6 but not Pms1. Proc Natl Acad Sci U S A. 101(25):9315-9320. doi:10. 1073/pnas.0305749101.
- Sundararajan R, Gellon L, Zunder RM, Freudenreich CH. 2010. Double-strand break repair pathways protect against CAG/CTG repeat expansions, contractions and repeat-mediated chromosomal fragility in Saccharomyces cerevisiae. Genetics. 184(1): 65-77. doi:10.1534/genetics.109.111039.
- Sznajder LJ, Swanson MS. 2019. Short tandem repeat expansions and RNA-mediated pathogenesis in myotonic dystrophy. Int J Mol Sci. 20(13):3365. doi:10.3390/ijms20133365.

- Sznajder LJ, Thomas JD, Carrell EM, Reid T, McFarland KN, Cleary JD, Oliveira R, Nutter CA, Bhatt K, Sobczak K, et al. 2018. Intron retention induced by microsatellite expansions as a disease biomarker. Proc Natl Acad Sci U S A. 115(16):4234–4239. doi:10.1073/pnas. 1716617115.
- Tian L, Gu L, Li GM. 2009. Distinct nucleotide binding/hydrolysis properties and molar ratio of MutSalpha and MutSbeta determine their differential mismatch binding activities. J Biol Chem. 284(17):11557-11562. doi:10.1074/jbc.M900908200.
- Usdin K, House NC, Freudenreich CH. 2015. Repeat instability during DNA repair: insights from model systems. Crit Rev Biochem Mol Biol. 50(2):142-167. doi:10.3109/10409238.2014.999192.
- van den Broek WJ, Nelen MR, Wansink DG, Coerwinkel MM, te Riele H, Groenen PJTA, Wieringa B. 2002. Somatic expansion behaviour of the (CTG)n repeat in myotonic dystrophy knock-in mice is differentially affected by Msh3 and Msh6 mismatchrepair proteins. Hum Mol Genet. 11(2):191-198. doi:10.1093/ hmg/11.2.191.
- Wheeler VC, Dion V. 2021. Modifiers of CAG/CTG repeat instability: insights from mammalian models. J Huntingtons Dis. 10(1): 123-148. doi:10.3233/JHD-200426.
- Williams GM, Surtees JA. 2015. MSH3 promotes dynamic behavior of trinucleotide repeat tracts in vivo. Genetics. 200(3):737-754. doi: 10.1534/genetics.115.177303.
- Yu X, Gabriel A. 1999. Patching broken chromosomes with extranuclear cellular DNA. Mol Cell. 4(5):873-881. doi:10.1016/S1097-2765(00)80397-4.
- Zhang Y, Saini N, Sheng Z, Lobachev KS. 2013. Genome-wide screen reveals replication pathway for quasi-palindrome fragility dependent on homologous recombination. PLoS Genet. 9(12): e1003979. doi:10.1371/journal.pgen.1003979.
- Zhao XN, Kumari D, Gupta S, Wu D, Evanitsky M, Yang W, Usdin K. 2015. Mutsbeta generates both expansions and contractions in a mouse model of the Fragile X-associated disorders. Hum Mol Genet. 24(24):7087-7096. doi:10.1093/hmg/ddv408.
- Zu T, Cleary JD, Liu Y, Banez-Coronel M, Bubenik JL, Ayhan F, Ashizawa T, Xia G, Clark HB, Yachnis AT, et al. 2017. RAN translation regulated by muscleblind proteins in myotonic dystrophy type 2. Neuron. 95(6):1292-1305.e5. doi:10.1016/j.neuron.2017. 08.039.
- Zu T, Gibbens B, Doty NS, Gomes-Pereira M, Huguet A, Stone MD, Margolis J, Peterson M, Markowski TW, Ingram MAC, et al. 2011. Non-ATG-initiated translation directed by microsatellite expansions. Proc Natl Acad Sci U S A. 108(1):260-265. doi:10.1073/ pnas.1013343108.

Editor: N. Rhind